REFERENCES

[1] H. A. Bethe, "Theory of diffraction by small holes," *The Physical Review*, vol. 66, p. 163, 1944.
[2] J. H. Davis, Unpublished Notes from Research Notebook No. 2, Electrical Engineering Research Laboratory, The University of Texas at Austin, June 18, 1971, p. 55.
[3] C. G. Montgomery, R. H. Dicke, and E. M. Purcell, *Principles of*

Microwave Circuits. New York: McGraw-Hill, p. 296f, 1948.
[4] C. E. Nelson, "Circularly polarized microwave cavity filters," *IRE Trans. Microwave Theory Tech.*, p. 136, 1957.
[5] J. C. Slater, *Microwave Electronics.* New York: Dover Publication, p. 147, 1969.
[6] R. L. Williams, "A three-cavity circularly polarized waveguide directional filter yielding a maximally flat response," *IRE Trans. Microwave Theory Tech.*, p. 324, 1962.

Helical Coupler from Rectangular-to-Circular Waveguide

C. READ PREDMORE, MEMBER, IEEE

Abstract—The very-large-array (VLA) radio telescope utilizes a low-loss TE_{01} circular waveguide transmission system. During the design of this system a coupler was developed which couples directly from a standard millimeter rectangular waveguide to the TE_{01}^C mode in highly over-moded circular waveguide. In contrast to previous couplers which used periodically spaced groups of coupling holes, this design wraps the rectangular waveguide in a helix around the circular waveguide to give a continuous array of coupling apertures for maximum coupling and a compact mechanical configuration. The helix angle is chosen to match the phase velocities of the rectangular and circular waveguide modes at a given frequency. In particular, couplers have been designed and fabricated which couple from WR-28 (26.5–40-GHz) and WR-22 (33–50-GHz) rectangular waveguides to the TE_{01}^C mode in 20- and 60-mm-diam circular waveguide.

I. INTRODUCTION

THE very-large-array (VLA) radio telescope, presently being constructed near Socorro, NM, will combine the signals from 27 paraboloid antennas. The antennas are each 25 m in diameter and are arranged in a Y-shaped pattern to provide the optimum sky coverage [1]. Nine antennas will be placed on each arm of the Y at distances from 40 m to 21 km from the intersection of the three arms. There are 24 fixed locations on each arm for various observing configurations, with 14 of those stations being within 2 km of the center. All of the antennas on an arm are connected to the control building near the center of the array by a single TE_{01}^C mode transmission system. This low-loss mode is achieved in a 60-mm-diam circular waveguide which has a helix lining of enameled copper wire for spurious mode suppression [2]–[4]. This waveguide mode has been studied for a number of decades [5] but has been brought to the production stage only recently in Japan and the United States [6].

Each antenna transmits local oscillator tones and a 200-MHz band received from astronomical sources to the control room in a 1-GHz band at a fixed frequency between 26 and 52 GHz. Weinreb *et al.* [7] describe the waveguide system in more detail. Since the losses in the circular waveguide are only 2.2–1.2 dB/km, between 26 and 52 GHz, the waveguide losses for the first 14 stations are less than 5 dB. Consequently, directional couplers with only loose coupling are required at those inner stations. It was desired to leave the couplers in place when the outer ten stations were being used. Since signals from those stations must propagate through the inner stations, the coupler insertion loss, return loss, and TE_{0n}^C ($n > 1$) mode generation must be quite good. Section II discusses the desired characteristics for coupling into the 60-mm waveguide and matches the possible coupler types to the system requirements. In Section III the helical coupler design will be discussed. Then the experimental results for 20- and 60-mm helical couplers will be presented.

II. DESIGN CRITERIA

The observing positions for the VLA antennas are clustered near the center of the Y with the first 14 stations within 2 km of the center. Beyond 2 km the spacing between stations increases from 400 m to 4 km. The waveguide loss is low so that no repeaters are required over the 21-km length. But, since the low loss does not dampen out interactions between system components such as couplers, which may be kilometers apart, the characteristics of the system components must be well chosen. Since the helix-lined waveguide will filter out TE_{mn}^C ($m > 0$) and TM_{mn}^C modes with a loss of >2000 dB/km, the prime considerations are the TE_{01}^C return loss and the TE_{01}^C–TE_{02}^C mode generation for a wave going through a coupler.

A coupler with an inner diameter the same as the rest of the circular waveguide will minimize these quantities since reflections and TE_{0n}^C ($n > 1$) mode generation are primarily caused by diameter changes [8]. Small-diameter couplers

TABLE I
COUPLER COMPARISON

	Coupling Length (m)	Overall Length (m)	$TE_{10}^{\square}$-$TE_{01}^{\bigcirc}$ Coupling (dB)	Coupling Variation in 1 GHz (dB)	$TE_{01}^{\bigcirc}$ Insertion Loss* (dB)	$TE_{01}^{\bigcirc}$ Return Loss (dB)	$TE_{01}^{\bigcirc}$-$TE_{02}^{\bigcirc}$ Mode Generation (dB)	$TE_{01}^{\bigcirc}$/$TE_{02}^{\bigcirc}$ Mode Discrimination (dB)
Phase Matched Coupler	0.4	2.4	-3	1	0.5	25	-30	30
60 mm Diameter Periodic Coupler	1.2	1.8	-26to-34	3	0.05	50	-50	10
60 mm Diameter Beam Splitter Coupler	0.06	0.2	-3	1	0.2to0.6	35	-17to-27	17 to 27
20 mm Diameter Helical Coupler	0.4	2.5	-13to-24	2	0.5	30	-30	30
60 mm Diameter Helical Coupler	0.4	1.0	-24to-32	3	0.05	50	-50	10

*Not including coupled power loss.

require circular cross-sectional tapers from the small diameter to the 60-mm diameter of the waveguide system [9], [10]. These tapers generate $TE_{02}^{\bigcirc}$ mode which can resonate between pairs of tapers in which the smaller diameter is cut off to the $TE_{02}^{\bigcirc}$ mode [11].

In the past coupling from the $TE_{10}^{\square}$ to the $TE_{01}^{\bigcirc}$ mode has been accomplished by making the waveguide dimensions such that the cutoff frequencies in the two waveguide modes are the same [12]. A circular waveguide diameter of 17.4 mm is required for phase matching to WR-28 (7.11 × 3.56 mm), and a 13.4-mm diameter is required for phase matching to WR-22 (5.59 × 2.79 mm) rectangular waveguide. If it was not possible to choose the waveguide dimensions to match the cutoff frequencies, it was still possible to use periodic coupling as described by Miller [13], [14]. However, for coupling between the axial magnetic fields, the number of coupling apertures in a given length is $1/\pi$ the number possible with a continuous coupling array. A third type of coupler is the quasi-optical beam splitter [15], [16] which consists of two 60-mm-diam waveguides which have a dielectric sheet at their intersection to couple out power by reflection. The helical coupler which wraps the rectangular waveguide around the circular waveguide in a spiral can be designed to phase match into any circular waveguide diameter which has a $TE_{01}^{\bigcirc}$ cutoff frequency lower than the $TE_{10}^{\square}$ cutoff frequency.

These various couplers are compared in Table I which lists the actual coupling length and the overall length when the coupler is used in a 60-mm-diam system. Then the $TE_{10}^{\square}$–$TE_{01}^{\bigcirc}$ coupling value and variation in coupling over the 1-GHz bandwidth required for the VLA are given. Next, the $TE_{01}^{\bigcirc}$ insertion loss, the $TE_{01}^{\bigcirc}$ return loss, and the $TE_{10}^{\bigcirc}$–$TE_{02}^{\bigcirc}$ mode generation are listed. The final quantity in the table is the $TE_{02}^{\bigcirc}$ mode discrimination, which is the ratio of the power coupled from the $TE_{10}^{\square}$ to $TE_{01}^{\bigcirc}$ mode to the power coupled from the $TE_{10}^{\square}$ to $TE_{02}^{\bigcirc}$ mode in the 1-GHz band centered on the coupler design frequency. For each of these couplers the $TE_{10}^{\square}$ return loss can be better than 23 dB and the coupler directivity better than 20 dB.

As can be seen from Table I, each type of coupler has different advantages which can be evaluated when selecting a coupler for a particular specification. While the phase-matched coupler which has a small diameter such as 13 mm and the beam-splitter coupler with a 60-mm diameter can couple as strong as −3 dB, they both have an unacceptable level of $TE_{01}^{\bigcirc}$–$TE_{02}^{\bigcirc}$ mode generation for the inner couplers of the VLA system. This is caused by the tapers associated with the phase-matched coupler, which also add 2 m in length and additional cost to the coupler. The $TE_{02}^{\bigcirc}$ mode generation is due to the intersecting 60-mm waveguide in the case of the beam splitter. This mode generation can be minimized at a particular frequency, but not over the octave band used in the VLA waveguide system [17]. A 60-mm-diam periodic coupler would have the required $TE_{01}^{\bigcirc}$ return loss and $TE_{01}^{\bigcirc}$–$TE_{02}^{\bigcirc}$ mode generation, but would have almost twice the overall length of the helical coupler and greater losses in the rectangular waveguide due to the longer length. The helical coupler offers the maximum coupling and most compact mechanical size in a 60-mm-diam coupler while achieving a high $TE_{01}^{\bigcirc}$ return loss and a low $TE_{01}^{\bigcirc}$–$TE_{02}^{\bigcirc}$ mode generation.

Beyond the inner 2 km of the VLA, stronger couplers are needed to compensate for the increasing waveguide loss. Phase-matched small-diameter couplers, 60-mm-diam beam-splitter couplers, and 20-mm-diam helical couplers are all being considered for the stronger coupling requirements.

III. COUPLER DESIGN

Once the circular waveguide diameter and channel frequencies are set by system requirements and the rectangular waveguide dimensions dictated by standard frequency bands, the number and size of the coupling apertures and the angle at which the rectangular waveguide is spiraled around the circular waveguide are determined. To optimize the VSWR and coupler directivity, the coupling slots are spaced an odd multiple of a quarter-wavelength apart along the axis of the circular waveguide. The arrangement of the coupling slots is shown in Fig. 1, which is a photograph of the helical coupler before the outer wall
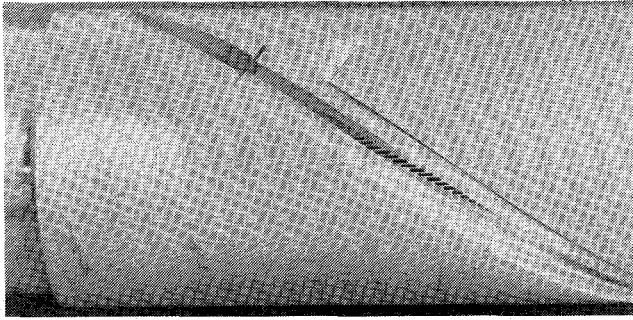
Fig. 1. Photograph of helical coupler from WR-28 to 60 mm. The outer cover of the rectangular waveguides has been left off to show the details of the coupling slots. At the end is a straight slot for adapting to standard WR-28 waveguide and a choke section for matching.
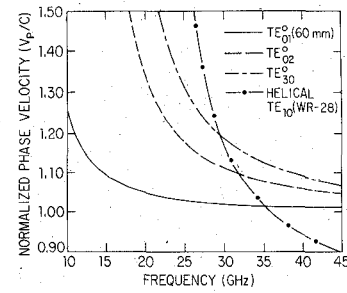

Fig. 2. Phase matching between the $TE_{10}^{\square}$ mode in helical WR-28 waveguide and the TE_{01}^{O}, TE_{02}^{O}, and TE_{03}^{O} modes in 60-mm-diam circular waveguide. The cutoff frequencies for those modes are 21.2, 6.09, 11.2, and 16.2 GHz, respectively.
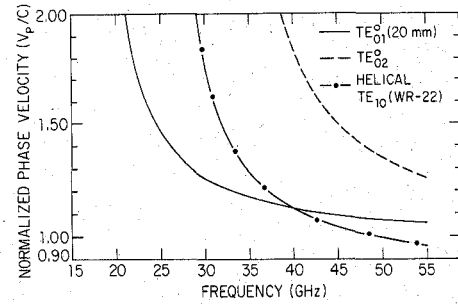

Fig. 3. Phase matching between the $TE_{10}^{\square}$ mode in helical WR-22 waveguide and the TE_{01}^{O} and TE_{02}^{O} modes in 20-mm-diam circular waveguide. The cutoff frequeocies for those modes are 26.7, 18.3, and 33.5 GHz, respectively.

of the rectangular waveguide was fabricated. The helical coupler allows a continuous array of coupling apertures by machining a rectangular waveguide in a spiral around the circular waveguide. The narrow wall of the rectangular waveguide is common with the outer wall of the circular waveguide and the outer wall of the rectangular waveguide is fabricated in another step. The details of the design are discussed in the remainder of this section.

A. Multihole Coupling Arrays

The treatment of multihole coupling arrays given by Levy [18] for coupling between identical waveguides has been generalized to the case of coupling between dissimilar waveguides. The coupling arrays used in the helical coupler have a large number of identical apertures with three or four smaller slots at each end for matching purposes. Although these smaller slots are accounted for in the actual design, they are neglected in the following analysis. The total effect of the multihole coupling array is found for 1) the forward-coupled wave from the $TE_{10}^{\square}$ to the TE_{0n}^{O} mode, 2) the reverse-coupled wave, and 3) for the reflected wave within the rectangular waveguide. The amplitudes for these three waves due to the coupling array are

$$A_1 = \sin\left[r \cdot (\phi_1 - \phi_2 - \varepsilon)/2\right]/\sin\left[(\phi_1 - \phi_2 - \varepsilon)/2\right] \tag{1}$$

$$A_2 = \sin\left[r \cdot (\phi_1 + \phi_2 + \varepsilon)/2\right]/\sin\left[(\phi_1 + \phi_2 + \varepsilon)/2\right] \tag{2}$$

and

$$A_3 = \sin\left[r \cdot (\phi_2 + \varepsilon)\right]/\sin(\phi_2 + \varepsilon) \tag{3}$$

where r is the number of coupling apertures, and ϕ_1, ϕ_2 are the electrical lengths along the circular waveguide axis between slots in the circular and rectangular waveguide, respectively. The phase shift in the rectangular waveguide due to the susceptance of the coupling aperture is typically 0.03 rad and is given by

$$\varepsilon = \tan^{-1} \rho \tag{4}$$

where ρ is the amplitude of the reflected wave in the rectangular waveguide as calculated in (9). The phase shift in the circular waveguide is negligible. The electrical lengths are given by

$$\phi_1 = 2\pi \cdot s/\lambda_g^O \tag{5a}$$

and

$$\phi_2 = 2\pi \cdot s/(\lambda_g^{\square} \cdot \cos\theta). \tag{5b}$$

The guide wavelengths $\lambda_g^O, \lambda_g^{\square}$ are for the TE_{0n}^{O} and $TE_{10}^{\square}$ modes, the slot spacing is s, and the helix angle is θ. At the coupler center frequency f_0 the helix angle is chosen so that

$$\phi_1 = \phi_2 + \varepsilon \tag{6a}$$

or

$$\cos\theta = 1/\lambda_g^{\square} \cdot (1/\lambda_g^O - \varepsilon/2\pi s)^{-1} \tag{6b}$$

which reduces to

$$\cos\theta = \lambda_g^O/\lambda_g^{\square} \tag{6c}$$

when the phase shift ε is zero. This condition, which gives the maximum forward coupling, is illustrated in Fig. 2. This figure shows the phase matching of a WR-28 waveguide to a 60-mm-diam circular waveguide. The phase velocities versus frequency are plotted for the $TE_{10}^{\square}$, TE_{01}^{O}, TE_{02}^{O}, and TE_{03}^{O} modes. The helix angle is chosen so that phase matching occurs at 35 GHz. Because of their higher cutoff frequencies, the rectangular waveguide is matched to the TE_{02}^{O} and TE_{03}^{O} modes at 32.5 and 27.8 GHz, respectively. The slot spacing along the circular waveguide axis is $\lambda_g^O/4$ at the center frequency. This makes

$$\phi_1 = \phi_2 + \varepsilon = \pi/2 \tag{7}$$

and minimizes the reverse-coupled wave (A_2) and the reflected wave (A_3) within the rectangular waveguide.

In Fig. 3 the phase matching of a WR-22 (5.6 × 2.8 mm) waveguide to 20-mm-diam circular waveguide is illustrated.

In this case the design frequency is 40 GHz. Also, for this design the $TE_{10}^{\square}$ cutoff frequency of 26.8 GHz is less than the TE_{02}^{O} cutoff frequency of 33.5 GHz so that the rectangular waveguide is not phase matched to the TE_{02}^{O} or higher TE_{0n}^{O} modes at any frequency. This greatly decreases the coupling into the TE_{0n}^{O} ($n > 1$) modes.

Since the coupling amplitude for a single slot does not vary rapidly with frequency, the bandwidth of the coupling is determined by the change in the electrical lengths ϕ_1, ϕ_2 as frequency varies and is expressed in (1). Even with the best calculations, a machined coupler may have errors of 1 percent in the peak coupling frequency f_0. At 35 GHz this shift is up to 20 percent of the 3-dB bandwidth. Fortunately, the coupler can be tuned to the correct frequency before the outer wall of the rectangular waveguide is fabricated. The tuning is accomplished by machining the outer wall of the cylinder in which the rectangular waveguide is milled. This decreases the rectangular waveguide width a and increases the cutoff frequency. As can be seen from Figs. 2 and 3, increasing the $TE_{10}^{\square}$ mode cutoff frequency increases the phase-matching frequency f_0. At 35 GHz, for the coupler described by Fig. 2, the tuning sensitivity is Δf_0 (GHz) = $9.4\Delta a$ (mm).

B. Calculation of Coupling Strength

The calculation of the coupling between two waveguides due to an aperture in a common wall follows that of Collin [19]. As shown in Fig. 1, the apertures are slots in the narrow wall of the rectangular waveguide with their longer dimension parallel to the axis of the circular waveguide. The magnetic polarizability for each slot, as well as the correction for the slot resonance frequency and finite wall thickness, are from the work of Cohn [20], [21]. The amplitude of the coupling between the $TE_{10}^{\square}$ and TE_{0n}^{O} modes is given by

$$C = \frac{\omega \mu_0}{2} h_z^{\square}(M_l \cos \theta) h_z^{O}. \tag{8}$$

The amplitude of the reflection in the rectangular waveguide due to the coupling slot is given by

$$\rho = \frac{\omega \mu_0}{2} (h_z^{\square})^2 (M_l \cos^2 \theta + M_w \sin^2 \theta). \tag{9}$$

The longitudinal magnetic fields $h_z^{\square}$ and h_z^{O} are the normalized fields at the coupling aperture for the modes being coupled and are given in the following equations:

$$h_z^{\square} = \left(\frac{2\lambda_0 \lambda_g^{\square}}{ab Z_0 (\lambda_{10}^{\square})^2} \right)^{1/2} (\text{Am}^{-1}\text{W}^{-1/2}) \tag{10}$$

$$h_z^{O} = \left(\frac{4\lambda_0 \lambda_g^{O}}{\pi D^2 Z_0 (\lambda_{0n}^{O})^2} \right)^{1/2} (\text{Am}^{-1}\text{W}^{-1/2}). \tag{11}$$

The free-space wavelength is λ_0, the guide wavelengths for the rectangular and circular waveguide modes are $\lambda_g^{\square}$ and λ_g^{O}, and the cutoff wavelengths are $\lambda_{10}^{\square}$ and λ_{0n}^{O}, respectively. The rectangular waveguide width and height are a and b, respectively, and the circular waveguide diameter is D. The impedance of free space is $Z_0 = 377 \, \Omega$.
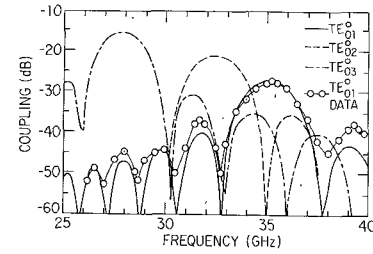

Fig. 4. Coupling between WR-28 and 60-mm-diam circular waveguide. The theoretical curves for the first three TE_{0n}^{O} modes are shown.

The angular frequency is ω and μ_0 is the permeability of free space. The magnetic polarizabilities parallel and normal to the slot axis are M_l and M_w, respectively.

Once the reflection and coupling due to a single aperture are determined, the total effect of the 100 to 150 slots is found. The coupling C of (8) is multiplied by A_1, A_2 to determine the coupled amplitudes, while ρ of (9) is multiplied by A_3 for the reflected wave within the rectangular waveguide.

Coupling amplitudes for the three waves are calculated over the frequency range for the rectangular waveguide which is being used for the coupling. It is necessary to account for an additional factor in the design by including the loss of the coupling slots. Measurements on the actual loss due to coupling into the circular waveguide were made on the rectangular waveguide as a function of the slot resonance frequency, and an empirical formula was fitted to these data and applied to the calculation of the coupler response versus frequency.

C. Minimizing TE_{02} Coupling

All of the TE_{0n}^{O} modes are circularly symmetric with only transverse currents on the wall, and consequently all of these modes have a low loss in the helix waveguide. Generation of both TE_{01}^{O} and TE_{0n}^{O} ($n > 1$) does not cause a problem until the TE_{0n}^{O} ($n > 1$) modes are reconverted to the TE_{01}^{O} mode by waveguide and joint diameter changes, or in other system components such as tapers between circular waveguides with different diameter (i.e., a 20–60-mm-diam taper).

Fig. 4 shows the theoretical coupling to the TE_{01}^{O}, TE_{02}^{O}, and TE_{03}^{O} modes for WR-28 to 60-mm coupler. Also shown are the experimental results of a coupler fabricated from the design data. The theory gives a good fit to the main coupling peak and the frequencies of the coupling nulls but does not exactly predict the height of the sidelobes. By using pairs of couplers, the coupling peaks of the TE_{02}^{O} and TE_{03}^{O} modes have been measured and are within 3 dB of the theory.

As was indicated in Fig. 2, the peak of the TE_{02}^{O} coupling occurs below the peak of the TE_{01} coupling, so the first null of the TE_{02}^{O} coupling is positioned at the center frequency of the coupler to minimize the mode coupling.

If the electrical lengths between slots are calculated for the $TE_{10}^{\square}$ and TE_{02}^{O} modes at the design frequency f_0, then the number of coupling slots r is chosen so that

$$r(\phi_1 - \phi_2 - \varepsilon) = \pm \pi. \tag{12}$$

Measurements of the beat between the TE_{01}^O and TE_{02}^O modes near f_0 indicate that the TE_{02}^O mode discrimination is about 10 dB as expected although TE_{02}^O generation in the tapers used is not known exactly. The TE_{03}^O and higher TE_{0n}^O modes are less of a problem since their reconversion to the TE_{01}^O mode in tapers is at least 10 dB weaker than that due to the TE_{02}^O mode and their losses in the circular waveguide are greater than 5 dB/km.

IV. EXPERIMENTAL RESULTS

The design techniques discussed in the previous section were developed over a period of two years, with several iterations of couplers needed before the final design was settled. The primary difficulty was the shape and size of the coupling apertures. Initially, circular holes were tried but they had very strong resonances due to the excitation of spurious modes within the circular waveguide. Finally, slots with about a 4:1 length-to-width ratio were used. Although the coupled power increases as the sixth power of the slot length, there is also an increasing loss from power coupled into other circular waveguide modes. For coupling from WR-28 waveguide into 60-mm-diam waveguide, the optimum slot length is almost $3\lambda_0/8$ at the design frequency.

Table II summarizes the mechanical parameters for three helical couplers. Listed are the dimensions for the rectangular waveguide, the cutoff frequencies for the $TE_{10}^\square$ and TE_{01}^O modes, and the design frequency. Next the helix angle and slot parameters are given. The slot parameters are the slot spacing, the total number of slots, and the slot length and width. Their actual coupling from the $TE_{10}^\square$ to the TE_{01}^O mode is shown in Figs. 4, 5, and 6. The coupling shown in these figures was measured by using a swept backward-wave oscillator whose output went through a precision attenuation and a broad-band isolator, before going into a rectangular-to-circular waveguide transition and then a taper to 20- or 60-mm diameter as required. A short section of helix-lined circular waveguide was used as a mode filter before the coupler. The coupler was followed by a circular waveguide termination. The coupling was measured with the substitution technique by recording comparison curves at various attenuator settings and then recording the coupling with no attenuation.

The TE_{01}^O insertion and return loss and the TE_{01}^O to TE_{02}^O mode generation listed in Table I were measured in a 60-mm-diam test line using the automatic waveguide test set developed by Weinreb et al. [7] and Parrish [22].

Fig. 5 shows the coupling response for a higher frequency coupler fabricated in WR-22 rectangular waveguide. The data from a 20-mm helical coupler are shown in Fig. 6. This coupler has stronger coupling because of the stronger h_z^O fields in the 20-mm-diam waveguide, and has a broader bandwidth due to the small number of holes (50) and the small change in the differential electrical length ($\phi_1 - \phi_2$) with frequency.

V. CONCLUSION

Couplers have been designed and fabricated to couple from the $TE_{10}^\square$ mode to the TE_{01}^O or other TE_{0n}^O modes in
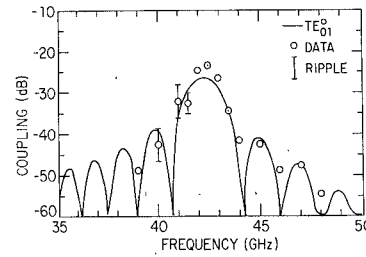
Fig. 5. Coupling between WR-22 and 60-mm-diam waveguide. The ripple below the peak coupling is due to a spurious mode.

TABLE II
HELICAL COUPLER PARAMETERS

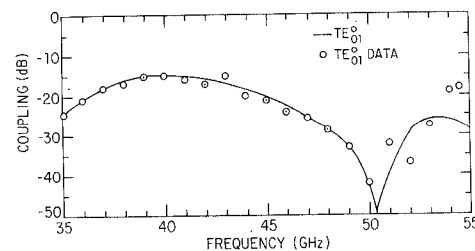|	WR-28 to 60 mm Diameter	WR-22 to 60 mm Diameter	WR-28 to 20 mm Diameter
Rectangular Waveguide Dimensions a, b (mm)	7.11, 3.56	5.59, 2.79	7.11, 3.56
$TE_{10}^\square$ Cutoff Frequency (GHz)	21.2	26.8	21.2
TE_{01}^O Cutoff Frequency (GHz)	6.09	6.09	18.3
Design Frequency (GHz)	35.1	42.3	40.0
Helix Angle θ	34.3°	36.6°	16.2°
Number of Slots	112	166	50
Slot Spacing (mm)	2.17	1.79	6.87
Slot Length (mm)	3.10	2.50	2.80
Slot Width (mm)	0.80	0.64	0.80

Fig. 6. Coupling between WR-28 and 20-mm-diam waveguide.

over-moded circular waveguide, over the octave band from 26 to 52 GHz. This design gives the maximum possible coupling, good directivity, excellent return loss, and a compact mechanical package. The theory can readily be extended to other frequencies and waveguide dimensions. Provision has been made to minimize the coupling to higher order TE_{0n}^{O} ($n > 1$) modes, or the coupler could be optimized as a TE_{0n}^{O} mode exciter for testing circular waveguide and circular waveguide components. With still smaller diameters, the helical couplers could be extended to stronger coupling and used as frequency-selective channel-dropping filters.

ACKNOWLEDGMENT

REFERENCES

[1] D. S. Heeschen, "The very large array," Sky and Telescope, vol. 49, pp. 344–351, June 1975.
[2] H. G. Unger, "Normal modes and mode conversion in helix waveguide," Bell Sys. Tech. J., vol. 40, pp. 255–280, Jan. 1961.
[3] K. Noda, K. Yamaguchi, and N. Suzuki, "Circular electric wave transmission through helix waveguide," Review of the Electrical Communication Laboratory, vol. 10, pp. 49–70, Jan./Feb. 1962.
[4] D. T. Young and W. D. Warters, "Precise 50–60 GHz measurements on a two-mile loop of helix waveguide," Bell Sys. Tech. J., vol. 48, p. 933, June 1968.
[5] S. E. Miller, "Waveguide as a communication medium," Bell Sys. Tech. J., vol. 33, pp. 1209–1247, June 1954.
[6] T. A. Abele, D. A. Alsberg, and P. T. Hutchison, "A high-capacity digital communication system using TE_{01} transmission in circular waveguide," IEEE Trans. Microwave Theory Tech., vol. MTT-23, pp. 326–333, April 1975.
[7] S. Weinreb, M. Ogai, A. Parrish, and R. Predmore, "Waveguide system for a very large antenna array," to be presented at the IEE International Conference on Millimetric Waveguide Systems, Nov. 9–12, 1976.
[8] H. E. Rowe and W. D. Warters, "Transmission in multimode waveguide with random imperfections," Bell Sys. Tech. J., vol. 41, pp. 745–768, May 1962.
[9] C. C. H. Tang, "Optimization of waveguide tapers capable of multimode propagations," IEEE Trans. Microwave Theory Tech., vol. MTT-9, pp. 442–452, Sept. 1961.
[10] H. G. Unger, "Circular waveguide taper of improved design," Bell Sys. Tech. J., vol. 37, pp. 1599–1647, 1958.
[11] A. P. King and E. A. Marcatili, "Transmission loss due to resonance of loosely-coupled modes in a multi-mode system," Bell Sys. Tech. J., vol. 35, pp. 899–906, 1956.
[12] A. P. King, "Status of low-loss waveguide and components at millimeter wavelengths," Microwave J., vol. 7, pp. 102–106, March 1964.
[13] S. E. Miller, "Coupled wave theory and waveguide applications," Bell Sys. Tech. J., vol. 33, pp. 661–719, May 1954.
[14] S. E. Miller, "On solutions for two waves with periodic coupling," Bell Sys. Tech. J., vol. 47, pp. 1801–1822, Oct. 1968.
[15] E. A. Marcatili and D. L. Bisbee, "Band splitting filter," Bell Sys. Tech. J., vol. 40, pp. 197–212, Jan. 1961.
[16] N. Suzuki, "A new band-splitting filter for guided-millimeter-wave transmission systems," IEEE Trans. Microwave Theory Tech., vol. MTT-24, pp. 237–241, May 1976.
[17] M. Ogai, private communication.
[18] R. Levy, "Directional couplers," in Advances in Microwaves, vol. 1. New York: Academic Press, 1966, pp. 115–211.
[19] R. E. Collin, Field Theory of Guided Waves. New York: McGraw-Hill, 1960.
[20] S. B. Cohn, "Determination of aperture parameters by electrolytic tank measurements," Proc. of the IRE, vol. 39, pp. 1416–1421, Dec. 1951.
[21] S. B. Cohn, "Microwave coupling by large apertures," Proc. of the IRE, vol. 40, pp. 696–699, June 1952.
[22] A. Parrish, Instruction Manual for VLA Circular Waveguide Test Set, NRAO Report, Green Bank, WV, Sept. 1974.